Coordinated Configuration Strategy of Multi-Energy Systems based on Capacity-Energy-Information Sharing

Zixuan Wang[a], Peng Li[a,*], Yue Zhou[b], Jianzhong Wu[b], Chunyan Zhang[c], Pingliang Zeng[d], Jiahao Wang[a], Youpeng Pan[a], Yunxing Yin[a]

[a] *School of Electrical and Electronic Engineering, North China Electric Power University, Baoding, Hebei, 071003, China*
[b] *School of Engineering, Cardiff University, Cardiff, CF24 0DP, UK*
[c] *State Grid Shanghai Municipal Electric Power Company, Shanghai, 200080, China*
[d] *School of Automation, Hangzhou Dianzi University, Hangzhou, Zhejiang, 310018, China*
* *Corresponding author.*
E-mail address: ncepulp@ncepu.edu.cn

***Abstract*—Multi-energy systems (MESs) integrate multiple energy vectors and contribute to energy efficient utilization, which have received considerable attention in the energy research field. However, regarding a MES with multi communities, the coordination among the communities has not been fully considered in its planning and configuration. Therefore, this paper proposes a coordinated configuration strategy for MES planning based on capacity-energy-information sharing. First, analysing the capacity, energy and information sharing mechanisms among communities, an improved energy hub (EH) model and hierarchical planning framework for MES is built. Moreover, a bilevel configuration model that coordinates the planning and operation stages is developed to design a MES, which is guided by the information sharing of communities. While the upper level model makes the optimal quantity and capacity configuration plan of communities with consideration of capacity sharing, the lower level model optimizes the best operation economy considering energy interactions in MES scheduling. Finally, a case study is carried out and simulation results show that, compared with the planning approaches in the reference cases, the proposed strategy contributes to a decrease in the MES planning costs and exhibits better performances in jointly considering the planning economy, robustness, carbon emissions and user benefits.**

Keywords—Multi-energy systems, integrated energy system, coordinated configuration, capacity-energy-information sharing, energy hub, planning and operation.

Nomenclature

Abbreviations			
AC	absorption chiller	IES	integrated energy system
DG	distributed generation	LHS	latin hypercube sampling
DR	demand response	MES	multi energy system
EC/GC	electric/gas air conditioner	MT	micro gas turbine
EH	energy hub	PV	photovoltaic
EDN/GDN/HDN	electric/gas/heat distribution network	T	transformer
ES/GS/HS/CS	electric/gas/heat/cold energy storage	WT	wind turbine
HE	heat exchanger	SADMM	synchronous alternating direction method of multipliers
Indices			
a/*b*	indices of additional/basic configuration values	*c*/*k*	indices of configuration capacity and quantity
i/*j*	indices of communities ($i, j \in \{1, 2, 3\}$).	*m*	index of equipment to be configured.
obj	index of planning objects.	*t*	index of hours (t=1,…, 24).
s	index of scenarios	*y*	index of typical seasons
u	index of energy forms ($u \in \{e, g, h, c\}$).		
Parameters			
D_y	total days of a year	T_{in}	load interruptible periods
$\bar{p}_u^t$ / p_u^t	energy prices before and after shifted DR	z^{obj}	life cycles of corresponding equipment [year]
$k_{u,in}$ / $k_{u,sft}$ / $k_{u,rpl}$	proportions of interrupted, shifted and replaced loads	α	unit treating cost of CO2 [¥/kg]
$k_{u'u}$	replacement efficiency between energy u and u'	γ_u	loss coefficient for energy interactions
$p_{u,cap}$ / $p_{u,in}$	capacity and energy compensation prices for interrupted DR [¥/kW h]	β_p / β_g / β_h / β_{mt}	carbon emission coefficients for electricity, gas, heat purchases and MT [kg/kWh]
$p_{i,om}^m$	operational maintenance coefficient [¥/kW h]	δ_{re}^{obj}	net residual rate of equipment, set as 8%

p_p^t / p_g^t / p_h^t	electric, gas and heat energy prices [¥/kW h]	ε_f^{obj}	fixed maintenance cost coefficient, set as 2%
$p_{u,sft}$	compensation coefficient for shifted DR [¥/kW h]	λ^{obj}	unit capacity investment cost [¥/(kW/kW h)]
r	discount rate, set as 6.7%	μ^{obj}	equivalent annual value factor
T	total scheduling periods of a day	l_{ij}^u	pipeline length of energy form u between communities i and j
Variables			
$E_{i,u}^{y,s,t}$	energy storage state [kW h]	$\varepsilon_{u,ij}^{y,s,t}$	direction of energy sharing
$P_{i,buy}^{y,s,t}$ / $G_{i,buy}^{y,s,t}$ / $H_{i,buy}^{y,s,t}$	electricity, gas and heat purchases [kW h]	$P_i^{m,y,s,t}$	output power of equipment m [kW]
$P_{i,u,in}^{y,s,t}$	actual load response amount for interrupted DR [kW h]	$P_{i,u,sft}^{y,s}$	total load change for time-shifted DR [kW h]
$P_{i,u,cap}$	reserved load amount for interrupted DR [kW h]	$P_{u,ij}^{y,s,t}$	energy sharing amount between community i and j
$x_{i,b,k}^m$ / $x_{i,a,k}^m$	basic/additional configuration quantity of equipment m	$x_{i,b,c}^m$ / $x_{i,a,c}^m$	basic/additional configuration capacity of equipment m

1. Introduction

With the gradual depletion of fossil energy and increasing concerns on environmental protection, the global energy supply is faced with great challenges [1]. How to alleviate the energy supply pressure and improve the energy utilization efficiency has become one of the most pressing issues to be solved in the energy field. In this context, multi-energy systems (MESs), which integrate various energy vectors, have emerged as an effective means of energy supply, transmission and consumption and have received considerable attention worldwide recently [2]. Many countries have developed plans and policies for building MESs, such as the "Internet +" smart energy plan of China [3], "Energylab Nordhavn" project for the European Union [4] and the "Energy independence and security" law for the United States [5].

A MES is an important carrier of Energy Internet, in which various energy production, transmission, conversion, storage and consumption parts are tightly integrated and coupled [6], thus facing considerable difficulties in its configuration planning and operation management. The MES planning plays an important role in the integration of diverse energy sources and loads, which has attracted a great deal of attention with many achievements worldwide. Modelling analysis is the basis for MES planning, where one of the most widely used modelling approach is the energy hub (EH) modelling. Energy hub was first proposed in [7] and introduced into the "Vision of Future Energy Networks" project for MES modelling, which offers a theoretical guidance for the following research into MESs. However, the traditional EH model contains only one energy coupling matrix, which does not allow for the integration of energy supply, conversion and storage parts. To address this, Ref. [8] proposed a standardized matrix modelling method for MESs based on graph theory, and Ref. [9] developed an energy circuit theory for heterogeneous energy flows modelling, both of the above extended the modelling approaches for MES planning. Moreover, terminal MES planning is usually geared to cases of buildings, communities and residential areas. For example, a distributed solar-biogas residential MES was designed in [10] for remote locations, which could reduce the dependency of MESs on battery storage systems. Ref. [11] proposed a novel optimization framework and model for the long-term investment planning of building multi-energy systems, which was able to optimize both energy and non-energy costs while considering building value. The above studies show that MES planning needs to consider the area resource and demand conditions, as well as the impact of multi factors on the planning economy. Furthermore, Ref. [12]-[14] carried out studies on the planning of community, park and district level MESs, respectively, which mainly aimed to optimize the quantity and capacity of equipment, as well as the laying of energy pipelines. In this paper, the research will focus on the configuration planning of a multi-community MES, which will be based on an improved EH model, and take into account the resource conditions and energy demands of different communities.

Meanwhile, with the ever-growing of diverse distributed energy sources and loads, it is noted that multiple uncertainty factors and demand-side participation, which could play an important role, should be considered into MES planning. In [15], probabilistic scenarios were adopted to establish a two-stage stochastic planning model for MES design, which considered the uncertainties of energy prices, emission factors and building demands. Ref. [16] further modelled the source-load uncertainties by a family of ambiguous probability distributions to present a data-driven two-stage robust stochastic programming model for MES capacity planning, while in [17], a bi-level joint-probabilistic programming method was developed for planning multi-regional energy system under different mitigation policies and uncertainties. Ref. [15]-[17] mainly performed studies on MES planning considering uncertainties from the perspective of probabilistic scenarios and stochastic optimization. However, the adopted uncertainty modelling measures in the above studies did not fully consider the robustness and randomness of energy sources and loads, which could have important implications for MES planning. On the role of energy demand side, some studies have introduced demand response into MES planning. Ref. [18] discussed the basic concepts and key issues of integrated demand response (IDR) in current research. On this basis, Ref. [19] proposed a two-stage stochastic model for the integrated design and operation of an energy hub, and integrated demand response programs were incorporated in the model to increase system flexibility, while in [20] and [21], both the price-based and incentive-based demand response were taken into account in MES planning and operation, respectively. However, the above works still lacked a coordinated consideration of various demand response measures in multi energy forms, and the effects of energy demand side were not fully taken into account in MES planning. Moreover, MES planning is usually optimized with the goals of economy, reliability, flexibility, etc., and it is necessary to consider the conflicting relationships between different objectives. Regarding the planning objectives balancing problem, Ref. [22] proposed a multi-actor regional energy system planning approach to achieve a balance of planning costs, land-use and visually impacted area, while in [23], a multi-objective decision-making model was constructed for renewable energy planning, which included the maximization of the technical score, environmental score, job creation, and economics. In [24], a quantitative evaluation index of renewable energies was introduced to propose a multi-objective capacity planning method for a MES, which aimed to minimize the economic cost and to maximize the complementarity rate of fluctuation simultaneously. However, planning robustness and user benefits were not taken into account in the above planning models. Although the above literatures studied the MES planning from different perspectives, most of them did not achieve a joint consideration of the aforementioned points, and developing a configuration model that coordinates multi factors in both the planning and operation stages is still a significant issue to be solved.

Moreover, the above studies related to terminal MES planning mainly focused on only one single community or energy building. For certain scenarios and cases, it is necessary to study the collaborative planning of a MES with several communities. Regarding to this, Ref. [25] proposed a novel low-carbon MES planning method, which considered the system privacy and environmental benefits while achieving a joint planning of regional and district MESs. For energy sharing among different MESs, Ref. [26] proposed a union optimal configuration strategy for a multi-microgrid energy system, which considered power interactions to improve system flexibility and planning economics, while in [27] and [28], multi energy interactions were further introduced into MESs planning and operation, respectively. Besides, regarding to building level MESs sharing, Ref. [29] presented a two-stage peer-to-peer energy sharing strategy for an energy building cluster to improve the system economics, while in [30], a game based bi-level energy sharing model was developed for residential photovoltaic (PV) panels planning, which achieved a balance between economic benefits and the reasonable installation of PV panels. However, in these studies, energy interactions were only considered in the MES energy management or the operation simulation of MES planning scheme. It is useful and necessary to expand energy sharing into the planning stage and further consider the information interactions in multi community planning, which we call as capacity and information sharing in this paper.

In summary, community sharing is playing a significant role in improving MES economics and flexibility, and the literature review reveals the gaps that the combined effects of capacity, energy and information sharing on energy supply and demand balance are not fully considered in present MES planning works. Moreover, current MES planning models still lack a joint consideration of multiple factors (uncertainty addressing, demand-side participation and multi-objective balancing) in both planning and operation stages, which has been quite important in MES planning, especially in the context of increasing energy supply and demand-side participation. In view of the above, the optimal planning problems of MES are far from being fully investigated. How to utilize the complementary advantages of various energy sources, how to give play to the multi dimension sharing measure in system optimization, and what planning strategies should be taken to coordinate multiple factors and obtain an optimal configuration plan remain open questions for MES planning.

Motivated by the research gaps, this paper proposes a bilevel coordinated configuration strategy for a MES with multi communities, which is based on capacity, energy and information sharing. By analysing the capacity, energy and information sharing mechanisms among communities, an improved energy hub model and hierarchical planning framework of MES is built.

On this basis, a bilevel configuration model is further developed, which effectively coordinates the planning and operation stages. Finally, the correctness and effectiveness of the proposed strategy are validated by a case study.

Compared with the existing works, the originality and main contributions of this paper are summarized as follows.

(1) This paper establishes an improved energy hub model for a MES, in which multi energy carriers, uncertainties, demand response and sharing measures are coordinated in model building. As a result, the proposed is generic for MES planning and operation and can promote the energy supply and demand balance.

(2) This paper proposes a coordinated configuration strategy for MESs based on multi-dimension sharing, which jointly considers capacity, energy and information sharing measures in both the planning and operation stages. Simultaneously, stochastic-robust-based scenarios are adopted to address source-load uncertainties and multi demand response measures are introduced to alleviate energy supply and demand pressure. The proposed strategy can effectively improve system flexibility by community interactions while reducing equipment configuration redundancy and MES planning costs.

(3) In this paper, a decomposition method combined with SADMM is implemented for solving the configuration model, and case studies are carried out by using a typical town area in China to validate the effectiveness and performances of the proposed strategy. Configuration and operation results analysis, as well as comparative analysis are performed for demonstration. As a result, the proposed strategy exhibits better performances in achieving a joint consideration of planning economy, robustness, carbon emissions and user benefits.

The remainder of the paper is constructed as follows. Section 2 analyses the capacity, energy and information sharing mechanisms, and develops an improved energy hub model and planning framework of MESs. Section 3 proposes a multi-dimension sharing based bilevel configuration strategy for MES planning. In Section 4, case studies are investigated to demonstrate the proposed strategy. Section 5 draws the conclusions.

2. Modelling and planning framework of MES

2.1 Sharing mechanisms analysis

In this paper, combined with the typical MES case with multi communities in Fig. 1, a structure of "collaborative planning and distributed operation" is adopted in this paper, that is, the configuration planning of the MES is carried out centrally, and the scheduling scheme of different communities will be formulated in a distributed optimization mode. Moreover, multi-dimensional sharing is further considered into the planning and operation of MES, and the sharing mechanisms are analysed as follows, which is closely related to the different organization modes in planning and operation stages.

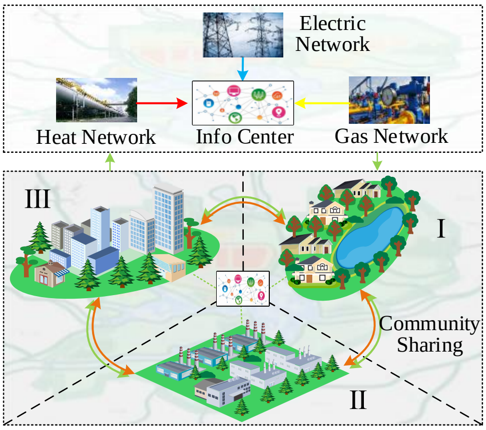

Fig.1 Structure of MES case with multi communities

2.1.1 Capacity sharing

The capacity sharing refers to that, when a community needs to configure the capacity of a certain equipment to meet its energy demands, and the configuration cannot be fully satisfied due to its own resources and site area limits, the part of "overflowing" capacity can be transferred to others for configuration, corresponding to the yellow part named "shared capacity" in Fig. 2. The capacity sharing measure will be considered for collaborative configuration of multi communities in the planning stage, which can effectively integrate the resource conditions and energy demands of communities with different regions and functional orientations, and is conducive to improving configuration efficiency.

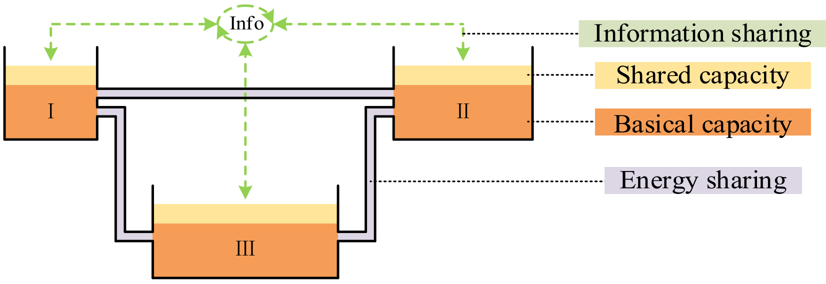

Fig.2 Diagram of community sharing

2.1.2 Energy sharing

The energy sharing refers to that, based on the differentiated energy supply and demand characteristics in the operation stage, a certain community can further satisfy its needs by performing energy purchases and sales with other communities, and it will also gain corresponding economic costs or benefits through energy interactions. As shown in the purple part among communities in Fig. 2, the shared energy mainly comprises two parts: one is the original surplus energy part of communities corresponding to base capacity, and the other is the energy part increased due to shared capacity. The energy sharing measure will be considered in the distributed operation scheduling of multi communities, which can achieve an interactive support and cooperative optimization of the communities, and promote the energy supply-demand matching and balancing.

2.1.3 Information sharing

The information sharing refers to that, various information (such as source-load data, equipment parameters and system status) of multi communities can be selectively shared with each other through a virtual "Info Center", which is correspondingly shown in green lines in Fig. 2. However, it should be noted that the info-sharing modes are quite different in the planning and operation stages. In the planning stage, multi communities are collaboratively configured by the constructor, thus forming a "complete information sharing" pattern; while a "partial information sharing" pattern is adopted in the operation stage owing to the distributed operation structure of MES, to protect the privacy and security of different communities. The information sharing measure can offer effective guidance for the implementation of capacity and energy sharing measures, and promote the collaborative planning and distributed operation of MESs.

2.2 Improved energy hub modelling

The diagram of a multi-community MES is shown in Fig. 1, and it is seen that the communities are interconnected by energy pipelines. For a certain community of which the structure is shown in Fig. 3, it consists of energy input (where EDN/GDN/ HDN stands for electric/gas/heat distribution networks), energy production (photovoltaic (PV) and wind turbine (WT)), energy conversion (transformer (T), heat exchanger (HE), micro gas turbine (MT), electric air conditioner (EC) and absorption chiller (AC)), energy storage (where ES/GS/HS/CS stands for electric/gas/heat/cold energy storage) and energy consumption (electric, gas, heating and cooling loads) parts. The equipment to be configured is highlighted in the dashed frame and the capacities of T and HE are assumed to be unlimited.

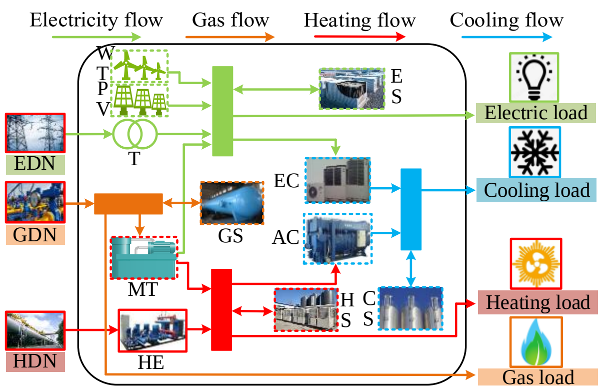

Fig.3 Diagram of community structure

The typical EH model of the community can be established through a coordination of energy input, production, conversion, storage and consumption parts, which is expressed in (A1) and simplified as follows.

$$L = C_{in}P_{in} + C_{de}P_{de} + C_{tr}P_{tr} + C_sP_s \tag{1}$$

where L represents the consumption variable matrix; P_{in}, P_{de}, P_{tr} and P_s denote the variable matrices of energy input, production, conversion, storage values, respectively; C_{in}, C_{de}, C_{tr} and C_s represent the corresponding coupling matrices, respectively.

Moreover, guided by the information sharing mode, the capacity and energy sharing measures are further introduced into the EH model: the capacity sharing gives additional items ΔP_{de}, ΔP_{tr} and ΔP_s to the corresponding variable matrices in the supply (right) side of (1) through the transfer of equipment configuration capacity; and the energy sharing can realize a transfer of energy demands in multi communities, to some extent, thus adding an equivalent modification ΔL to the matrix L in the demand (left) side of (1). In addition, considering that the uncertainties introduced by distributed energy sources and loads, and the adopted demand response measures, will also exert effects on the balance of energy supply and demand, corresponding modifications ξ_{de}, ξ_L and ΔL_{dr} of energy production, consumption items are added in the EH modeling, respectively. In summary, an improved EH model is developed below to jointly take into account the sharing measures, uncertainties and demand response.

$$\bar{L} + \Delta L + \Delta L_{dr} + \xi_L = C_{in}P_{in} + C_{de}(\bar{P}_{de} + \Delta P_{de} + \xi_{de}) + C_{tr}(P_{tr} + \Delta P_{tr}) + C_s(P_s + \Delta P_s) \tag{2}$$

where $\bar{L}$ and $\bar{P}_{de}$ represent the predicted power matrices of load and distributed energy sources.

In general, the multidimensionality of the improved EH modelling is reflected mainly in the following aspects: 1) multi energy vectors (electric, gas, heat and cold) and energy parts (energy input, production, conversion, storage and consumption); 2) multi uncertainties (randomness and volatility of DGs and loads) and demand response measures (response measures of multi energy loads); 3) multi sharing measures among communities (capacity, energy and information sharing).

2.3 Hierarchical planning framework of MES

Based on the sharing mechanism and improved EH model, a hierarchical planning framework is built for the design of MES, which is shown in Fig. 4.

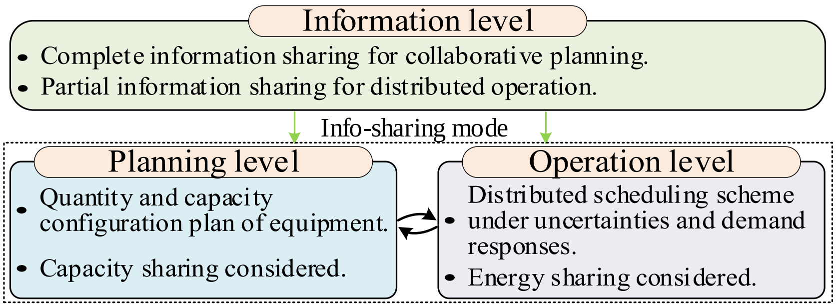

Fig.4 Hierarchical planning framework of MES

The framework mainly comprises planning, operation and information levels for MES configuration. While the planning level collaboratively makes the optimal quantity and capacity configuration plan taking into account the capacity sharing, the operation level considers the energy sharing measures and distributedly optimizes the best scheduling scheme under uncertainties and demand responses. Besides, the above two levels are both guided by the different info-sharing modes in the information level, to achieve a better coordination of planning and operation through iteration.

3. Multi-dimension sharing based bilevel configuration model of MES

Following the above hierarchical planning framework, here we give a bilevel configuration strategy based on multi-dimension sharing to design a MES with multi communities.

3.1 Upper level: configuration optimization

The decision making of the upper level problem contains three parts: 1) calculating the equipment capacity (x_b, base value) to be configured in a certain community according to its own needs; 2) determining the shared configuration capacity (x_a, added value) considering the needs of other communities; 3) planning the pipelines configuration (x_{ij}, 0-1 variable) among communities.

The objective function (3) of upper level model is to minimize the total annual cost C_{total} of MES planning, including configuration cost and operation cost C_{op} (detailed in Section 3.2), and configuration cost consists of the investment cost C_{inv}, fixed maintenance cost $C_{om,f}$ and equipment residual value C_{re}, which are expressed in (4)-(6), respectively.

$$\min C_{total} = \min_{x_b, x_a, x_p} \left(C_{inv} + C_{om,f} + C_{op} - C_{re} \right) \tag{3}$$

$$C_{inv} = \sum_{i} \sum_{m\in\Omega_m} \mu^m \lambda^m (x_{i,b,k}^m x_{i,b,c}^m + x_{i,a,k}^m x_{i,a,c}^m) + \sum_{ij} \sum_{u} \mu^u \lambda^u x_{ij}^u l_{ij}^u \tag{4}$$

$$C_{om,f} = \sum_{i} \sum_{m\in\Omega_m} \varepsilon_f^m \lambda^m (x_{i,b,k}^m x_{i,b,c}^m + x_{i,a,k}^m x_{i,a,c}^m) + \sum_{ij} \sum_{u} \varepsilon_f^u \lambda^u x_{ij}^u l_{ij}^u \tag{5}$$

$$C_{re} = \sum_{i} \sum_{m\in\Omega_m} \delta_{re}^m \lambda^m (x_{i,b,k}^m x_{i,b,c}^m + x_{i,a,k}^m x_{i,a,c}^m) / z^m + \sum_{ij} \sum_{u} \delta_{re}^u \lambda^u x_{ij}^u l_{ij}^u / z^u \tag{6}$$

$$\begin{cases} m \in \Omega_m = \{PV, WT, MT, EC, AC, ES, GS, HS, CS\} \\ u \in \{e, g, h, c\}, \quad obj \in \{m, u\}, \quad i, j \in \{1,2,3\}, i \neq j \end{cases} \tag{7}$$

$$\mu^{obj} = r(1+r)^{z^{obj}} / [(1+r)^{z^{obj}} - 1] \tag{8}$$

where investment cost refers to the one-time cost of equipment purchase; fixed maintenance cost refers to the cost of performing fixed maintenance on the energy equipment in a year; equipment residual value refers to the value that can be recovered when the equipment reaches its service life. Ω_m is the set of equipment to be configured; *u* and *obj* denote a certain energy form and planning object, respectively; μ^{obj}, ε_f^{obj}, δ_{re}^{obj}, z^{obj} and λ^{obj} denote the equivalent annual value factor, maintenance coefficient, net residual rate, life cycle and unit investment cost of *obj*, respectively; l_{ij}^u is the pipeline length of energy form *u* between community *i* and *j*; *r* is the discount rate; $x_{i,b,k}^m$ and $x_{i,b,c}^m$ are the basic configuration quantity and capacity of equipment *m* in community *i*; and $x_{i,a,k}^m$ and $x_{i,a,c}^m$ are the additional configuration parts to be shared in operation stage.

Considering the actual site limitations and energy structure, the constraints for upper level modeling include equipment quantity and capacity constraints (9) and energy supply and demand constraints (10), which are as follows:

$$\begin{cases} 0 \le x_{i,b,k}^m \le K_{i,b,\max}^m, \ 0 \le x_{i,a,k}^m \le K_{i,a,\max}^m \\ 0 \le x_{i,b,c}^m \le C_{i,b,\max}^m, \ 0 \le x_{i,a,c}^m \le C_{i,a,\max}^m \end{cases}, \ i \in \{1,2,3\} \tag{9}$$

$$\sum_{m\in\Omega_m^c} (x_{i,b,k}^m x_{i,b,c}^m + x_{i,a,k}^m x_{i,a,c}^m) \eta^m > L_{i,s}^c, \ s \in S \tag{10}$$

where $K_{i,b,\max}^m$ and $C_{i,b,\max}^m$ are the upper limits of basic configuration quantity and capacity; $K_{i,a,\max}^m$ and $C_{i,a,\max}^m$ are the upper limits of additional configuration quantity and capacity; $\Omega_m^c = \{EC, AC, CS\}$, and η^m denotes the conversion efficiency of equipment *m*; $L_{i,s}^c$ is the cooling load power of community *i*; *S* is the typical set of scenario *s*.

3.2 Lower level: operation optimization

In this level, based on the configuration plan and information sharing mode, the procedures for MES operation optimization can be divided into two parts: 1) allocating the shared capacity among communities according to their energy supply and demand situations; 2) optimizing the MES scheduling scheme with the consideration of uncertainty addressing, demand response and energy sharing.

3.2.1 Uncertainty characterization

In this paper, we consider the uncertainties introduced by the distributed energy sources (PV and WT outputs) and energy demands (electric, gas, heating and cooling loads). Robust concept is combined with the stochastic optimization approach to deal with the source-load uncertainties, which are represented by a set of typical scenarios. The specific processing procedures consist of scenario sampling, sorting, screening and reduction, which are correspondingly shown in (11)-(14).

$$\begin{cases} \xi_{mn} = F_m^{-1}\left(r_{mn} / N + (n-1)/N\right) \\ S_0 \Leftrightarrow S_0(\xi_1, \xi_2, \cdots, \xi_m) \to S_0(\xi_1^{'}, \xi_2^{'}, \cdots, \xi_m^{'}) \Leftrightarrow S \end{cases} \tag{11}$$

$$\begin{cases} S(\xi_1; \xi_2; \cdots; \xi_N) \underset{re-sorting}{\to} S_1(\xi_p; \xi_o; \cdots; \xi_q) \\ d_n = \sum_{j=i+1}^{m} (\xi_{nj} - \xi_{0j}) - \sum_{j=1}^{i} (\xi_{nj} - \xi_{0j}) \\ 1 \le o, p, q, n \le N \end{cases} \tag{12}$$

$$S_2 = S_1\left([N_\Gamma - N_1/2 + 1, N_\Gamma + N_1/2]\ ,\ 1{:}\ m\right) \tag{13}$$

$$\begin{cases} S_2(\xi_1; \xi_2; \cdots; \xi_N) \xrightarrow[reduction]{d_{ij}} S_3(\zeta_1; \zeta_2; \cdots; \zeta_{N'}) \\ d_{ij} = \left\| (\xi_{i1}, \xi_{i2}, \cdots, \xi_{im}) - (\xi_{j1}, \xi_{j2}, \cdots, \xi_{jm}) \right\| \end{cases} \tag{14}$$

Equation (11) stands for the stratified sampling and disturbed sorting, in which an initial sampling matrix S_0 of $N \times m$ is generated by Monte-Carlo Simulation, and the elements of each column in S_0 are rearranged to obtain S; scenario sorting is shown in (12), while the robust distance between a sampled scenario $(\xi_{n1}, \xi_{n2}, \cdots, \xi_{nm})$ and original typical scenario $(\xi_{01}, \xi_{02}, \cdots, \xi_{0m})$ is defined as $d_{n,robust}$, scenario re-sorting is performed to obtain S_1 according to their robust distances; scenario screening is performed in (13) to select N_1 scenarios from S_1 to obtain a robustness-based matrix S_2; finally, a backward scenario-reduction algorithm is used for scenario reduction to obtain S_3 in (14), of which the specific steps are detailed in [31]. ξ_{mn} is the n-th sampling value of a random vector ξ_m, obtained by its inverse function $F_m^{-1}(\cdot)$; r_{mn} is a random variable with uniform distribution in [0,1]; d_n is the robust distance between a sampled scenario and the original typical scenario; Γ is the robustness parameter and $\Gamma \in [0,1]$; d_{ij} is the Euclidean distance between scenario i and j; S_3 is the final stochastic-robust-based scenario set of $N' \times m$.

3.2.2 Integrated demand response modelling

In this paper, multiple DR measures are considered into the operation optimization, corresponding to the part of ΔL_{dr} in the improved EH model (2). Based on our previous work in [21], the shifted, replaced and interrupted DR are jointly coordinated in (15), and the response models are stated in (16)-(18), respectively.

$$\Delta L_{dr} = L_{fix} + L_{sft} + L_{rpl} + L_{in} - \bar{L} \tag{15}$$

$$\begin{cases} L_{u,sft}^t = k_{u,sft} \bar{L}_u^t + \Delta L_{u,sft}^t,\ 0 \le |\Delta L_{u,sft}^t| \le L_{u,sft,\max}^t \\ \Delta L_{u,sft}^t = k_{u,sft} \bar{L}_u^t \sum_{t'} [E_u(t,t') \cdot (p_u^t - \bar{p}_u^t) / \bar{p}_u^t] \end{cases} \tag{16}$$

$$\begin{cases} L_{u,rpl}^t = k_{u,rpl} \bar{L}_u^t + \Delta L_{u,rpl}^t,\ 0 \le |\Delta L_{u,rpl}^t| \le L_{u,rpl,\max}^t \\ \Delta L_{u,rpl}^t = \sum_{u' \ne u} k_{u'u} k_{u',rpl} \bar{L}_{u'}^t \end{cases} \tag{17}$$

$$L_{u,in}^t = k_{u,in} \bar{L}_u^t - \Delta L_{u,in}^t,\ \Delta L_{u,in}^t \le L_{u,in,\max}^t,\ t \in T_{in} \tag{18}$$

where $u \in \{e, g, h, c\}$; T is the total scheduling period, $t, t' \in T$; L_{fix} is the fixed load matrix; L_{sft}, L_{rpl} and L_{in} represent the corresponding matrices of response loads after DR; $k_{u,sft}$, $k_{u,rpl}$ and $k_{u,in}$ denote the proportion coefficients; $k_{u'u}$ denotes the replacement efficiency between energy u and u'; $\Delta L_{u,sft}^t$, $\Delta L_{u,rpl}^t$ and $\Delta L_{u,in}^t$ are the load variations; $L_{u,sft,\max}^t$, $L_{u,rpl,\max}^t$ and $L_{u,in,\max}^t$ are their corresponding upper limits; E_u is the energy price elasticity matrix; $\bar{p}_u^t$ and p_u^t are the energy prices before and after shifted DR, and only electric and gas loads are considered in shifted DR; T_{in} is the load interruptible period set.

3.2.3 Multi-community coordinated scheduling model

In the lower level model, the objective function of annual operation cost C_{op} is defined in (19), including the purchase cost C_{buy}, operational maintenance cost C_{om}, environmental cost C_{ep}, demand response cost C_{dr} and transmission loss cost C_{ls}, which are stated in (20)-(24), respectively.

$$
\begin{aligned}
\min C_{op} &= \min(C_{buy} + C_{om} + C_{ep} + C_{dr} + C_{ls}) \\
&= \sum_{y \in Y} \theta_y D_y \sum_{s \in S_3} Pr_s (\sum_i (C_{i,buy}^{y,s} + C_{i,om}^{y,s} + C_{i,ep}^{y,s} + C_{i,dr}^{y,s}) + C_{ls}^{y,s})
\end{aligned} \tag{19}
$$

$$
C_{i,buy}^{y,s} = \sum_t (p_p^t P_{i,buy}^{y,s,t} + p_g^t G_{i,buy}^{y,s,t} + p_h^t H_{i,buy}^{y,s,t}) \tag{20}
$$

$$
C_{i,om}^{y,s} = \sum_t \sum_{m \in \Omega_m} p_{i,om}^m x_{i,b,k}^m P_i^{m,y,s,t} \tag{21}
$$

$$
C_{i,ep}^{y,s} = \alpha \sum_t (\beta_p P_{i,buy}^{y,s,t} + \beta_g G_{i,buy}^{y,s,t} + \beta_h H_{i,buy}^{y,s,t} + \beta_{mt} P_i^{mt,y,s,t}) \tag{22}
$$

$$
C_{i,dr}^{y,s} = \sum_u (p_{u,sft} P_{i,u,sft}^{y,s} + p_{u,cap} P_{i,u,cap} + \sum_{t \in T_{in}} p_{u,in} P_{i,u,in}^{y,s,t}) \tag{23}
$$

$$
C_{ls}^{y,s} = \sum_t \sum_{ij} \sum_u p_u^t \gamma_u P_{u,ij}^{y,s,t} / 2 \tag{24}
$$

where purchase cost refers to the cost of purchasing electricity, natural gas and heat energy from the energy networks; operational maintenance cost refers to the cost of performing daily maintenance on the energy equipment; environmental cost refers to the cost of treating CO2 emissions; demand response cost refers to the user compensation costs owing to load change, including shifted and interrupted DR costs; transmission loss cost refers to the cost of energy interactions among communities. D_y is the total days of a year, and θ_y is the proportion of a typical season y; Pr_s is the probability of scenario s; $P_{i,buy}^{y,s,t}$, $G_{i,buy}^{y,s,t}$ and $H_{i,buy}^{y,s,t}$ are the electricity, gas and heat purchases of community i, and p_p^t, p_g^t and p_h^t are the corresponding prices; $p_{i,om}^m$ and $P_i^{m,y,s,t}$ are the operational maintenance coefficient and output power of equipment m; α is the unit treating cost of CO2; β_p, β_g, β_h and β_{mt} are the equivalent carbon emission coefficients. Moreover, based on user benefit considerations, demand response cost is taken into account for user compensations. $P_{i,u,sft}^{y,s}$ and $p_{u,sft}$ are the total change and compensation coefficient of load u for shifted DR; $p_{u,cap}$ and $p_{u,in}$ are the capacity and energy compensation prices for interrupted DR; $P_{i,u,cap}$ and $P_{i,u,in}^{y,s,t}$ are the reserved and actual response amount of load u; and compensation costs are not considered for replaced DR in this paper. $P_{u,ij}^{y,s,t}$, p_u^t and γ_u are the energy sharing amount, price and loss coefficient.

The constraints in lower level modeling comprise the energy balance constraints (25), purchase constraints (26), equipment constraints (27), sharing constraints (28) and DR constraints.

$$
\begin{aligned}
& L_{i,fix}^{y,s,t} + L_{i,sft}^{y,s,t} + L_{i,rpl}^{y,s,t} + L_{i,in}^{y,s,t} + \sum P_{ij}^{y,s,t} + \xi_L^{y,s,t} \\
&= C_{i,in} P_{i,in}^{y,s,t} + C_{i,de} (\bar{P}_{i,de}^{y,s,t} + \sum \Delta P_{ij,de}^{y,s,t} + \xi_{de}^{y,s,t}) \\
&+ C_{i,tr} (P_{i,tr}^{y,s,t} + \sum \Delta P_{ij,tr}^{y,s,t}) + C_{i,s} (P_{i,s}^{y,s,t} + \sum \Delta P_{ij,s}^{y,s,t})
\end{aligned} \tag{25}
$$

$$
0 \le P_{i,buy}^{y,s,t} \mid G_{i,buy}^{y,s,t} \mid H_{i,buy}^{y,s,t} \le P_{i,buy,\max} \mid G_{i,buy,\max} \mid H_{i,buy,\max} \tag{26}
$$

$$
\begin{cases}
0 \le P_i^{m,y,s,t} \le P_{i,\max}^m + \sum \Delta P_{ij}^{m,y,s,t} \\
E_{i,u,\min} \le E_{i,u}^{y,s,t} \le E_{i,u,\max},\ E_{i,u}^{y,s,0} = E_{i,u}^{y,s,24}
\end{cases} \tag{27}
$$

$$
\begin{cases}
-P_{u,ij,\max} \le \varepsilon_{u,ij}^{y,s,t} P_{u,ij}^{y,s,t} \le P_{u,ij,\max} \\
\sum_i \sum_{j \ne i} \varepsilon_{u,ij}^{y,s,t} P_{u,ij}^{y,s,t} = 0
\end{cases} \tag{28}
$$

where $i, j \in \{1,2,3\}, i \ne j$; $P_{ij}^{y,s,t}$ is the load modification matrix decided by energy sharing; $\Delta P_{ij,de}^{y,s,t}$, $\Delta P_{ij,tr}^{y,s,t}$ and $\Delta P_{ij,s}^{y,s,t}$ are the modification matrices over the corresponding parts decided by capacity sharing; $P_{i,buy,\max}$, $G_{i,buy,\max}$ and $H_{i,buy,\max}$ are the upper limits of energy purchases; $P_{i,\max}^m$ is the upper output limit of equipment m; $E_{i,u}^{y,s,t}$, $E_{i,u,\max}$ and $E_{i,u,\min}$ are the energy storage state and its upper and lower limits; $\varepsilon_{u,ij}^{y,s,t}$ and $P_{u,ij,\max}$ are the direction and upper limit of energy sharing; and the DR constraints are presented in (16)-(18).

3.3 Solution methodology

The established model is a mixed-integer linear programming problem with hierarchical structure, and the communities are coupled through energy interactions in operation scheduling. Therefore, a decomposition method combined with SADMM is implemented for model solving.

3.3.1 Benders decomposition algorithm

Considering the optimization problem proposed in Section 3.1 and 3.2, which can be simply expressed as follows:

$$\begin{cases} \min C_{total} = \min f(x_{up}) + g(x_{up}, x_{low}) \\ s.t. \quad G(x_{up}) \le 0 \\ \qquad G(x_{up}, x_{low}) \le 0 \\ \qquad G(x_{low}) \le 0 \\ \qquad H(x_{low}) = 0 \end{cases} \tag{29}$$

where $f(x_{up})$ and $g(x_{up}, x_{low})$ represent the main and sub problems, respectively, and x_{up} and x_{low} are the corresponding decision variables; $G(x_{up})$ denotes the inequality constraints of main problem (equation (9)-(10)); $G(x_{up}, x_{low})$ denotes the coupling constraints of main and sub problems (equation (27)); $H(x_{low})$ and $G(x_{low})$ denote the equality and inequality constraints of sub problem (equation (25), (26) and (28)). The steps to solve the problem using the Benders decomposition algorithm are as follows.

a) Initialization

Set the iteration number *kk*=1, the lower bound of the objective function $C_{total}^{\min(1)} = -\infty$, the decision variable of main problem $x_{up} = x_{up}^{(1)}$.

b) Sub problem solving

The solution model of the sub problem is shown in (30), where $x_{up}^{(kk)}$ is the solution of main problem in the iteration *kk*, and is regarded as a constant value.

$$\begin{cases} \min g(x_{up}^{(kk)}, x_{low}) \\ s.t. \quad G(x_{up}^{(kk)}, x_{low}) \le 0 \\ \qquad G(x_{low}) \le 0 \\ \qquad H(x_{low}) = 0 \end{cases} \tag{30}$$

If the sub problem is feasible, obtain the optimal solution $x_{low}^{(kk)}$ and update the upper bound of the objective function $C_{total}^{\max(kk)}$. Then construct the Benders cut constraints (31), where Z is the intermediate variable and $\lambda^{(kk)}$ is the dual multiplier of coupling constraints $G(x_{up}, x_{low})$.

$$g(x_{up}^{(kk)}, x_{low}^{(kk)}) + \lambda^{(kk)} G(x_{up}, x_{low}^{(kk)}) \le \mathrm{Z} \tag{31}$$

If the sub problem is not feasible, introduce the relaxation variable *S* and construct the following virtual sub problem (32). Then solve the virtual sub problem and obtain the Benders cut constraints (33), where *S** is the intermediate variable of objective function in (32).

$$\begin{cases} \min S \\ s.t. \quad G(x_{up}^{(kk)}, x_{low}) - S \le 0 \\ \qquad G(x_{low}) \le 0 \\ \qquad H(x_{low}) = 0 \end{cases} \tag{32}$$

$$S^* + \lambda^{(kk)} G(x_{up}, x_{low}^{(kk)}) \le 0 \tag{33}$$

c) Optimality test of solution

If the difference between the upper bound $C_{total}^{\max(kk)}$ and lower bound $C_{total}^{\min(kk)}$ is less than the convergence gap ε, that is, $\left| C_{total}^{\max(kk)} \text{-} C_{total}^{\min(kk)} \right| \le \varepsilon$, stop the iteration and output the optimal solution, otherwise add the Benders cut constraints to the main problem and continue the iteration.

d) Main problem solving

Update the iteration number kk+1, and the solution model of the main problem is shown in (34), where $x_{low}^{(kk)}$ is the solution of sub problem in the iteration kk, and is regarded as a constant value. Then obtain the optimal solution $x_{up}^{(kk+1)}$ and update the lower bound of the objective function $C_{total}^{\min(kk+1)}$, and continue the step b) Sub problem solving in iteration kk+1.

$$\begin{cases} \min f(x_{up}) + Z \\ s.t. \quad G(x_{up}) \le 0 \\ \qquad g(x_{up}^{(kk)}, x_{low}^{(kk)}) + \lambda^{(kk)} G(x_{up}, x_{low}^{(kk)}) \le Z \\ \qquad S^* + \lambda^{(kk)} G(x_{up}, x_{low}^{(kk)}) \le 0 \end{cases} \tag{34}$$

3.3.2 SADMM based distributed operation

In the operation stage, the communities are coupled through energy interactions (equation (28)), and therefore, synchronous alternating direction method of multipliers (SADMM) [32] is introduced into the sub problem to decouple the equality constraints, to realize the synchronous and distributed operation scheduling of multi communities.

Taking the energy interaction power as the coupling variables, and let $x_{low,i,ei}$ and $x_{low,i}$ denote the interaction and total decision variables of community i. Combined with (19), the sub problem (30) can be expressed as (35), where $g_i(\bullet)$ denotes the operation cost of community i, and $g_{cp}(\bullet)$ denotes the total transmission loss cost; $G_i(\bullet)$ and $H_i(\bullet)$ denote the independent constraints of community i, and $H_{cp}(\bullet)$ denotes the energy interaction coupling constraints.

$$\begin{cases} \min g(x_{low}) \\ = \min\left[\sum g_i(x_{low,i}) + g_{cp}(x_{low,1}, x_{low,2}, x_{low,3})\right] \\ s.t. \quad G_i(x_{low,i}) \le 0 \\ \qquad H_i(x_{low,i}) = 0 \qquad\qquad , i \in \{1,2,3\} \\ \qquad H_{cp}(x_{low,1}, x_{low,2}, x_{low,3}) \\ \qquad = x_{low,1,ei} + x_{low,2,ei} + x_{low,3,ei} = 0 \end{cases} \tag{35}$$

The iteration procedure of SADMM can be constructed as follows. ρ is the penalty factor, and $x_{low,ref,ei}^{nn+1}$ is the reference value in the iteration nn+1; μ_i^{nn} and μ_i^{nn+1} are the intermediate variables.

$$\begin{cases} x_{low,i}^{nn+1} = \arg\min\Big[g_i(x_{low,i}) + g_{cp}(x_{low,i}, x_{low,-i}^{nn}) \\ \qquad + \dfrac{\rho}{2}\left\| x_{low,i,ei} - x_{low,ref,ei}^{nn} + \mu_i^{nn} \right\|_2^2 \Big] \\ x_{low,ref,ei}^{nn+1} = \left(x_{low,i,ei}^{nn+1} - \sum x_{low,-i,ei}^{nn+1} \right) / 2 \\ \mu_i^{nn+1} = \mu_i^{nn} + (x_{low,i,ei}^{nn+1} - x_{low,ref,ei}^{nn+1}) \\ i \in \{1,2,3\}, \ \rho > 0 \end{cases} \tag{36}$$

To sum up, the procedures of the bilevel configuration problem solving are as follows. First, the Benders decomposition algorithm is adopted to decompose the model into a bilevel optimization problem with iterations of main and sub problems. Moreover, the SADMM is utilized for the distributed operation scheduling of multi communities in sub problems. The Gurobi solver is called for model solving of main and sub problems based on MATLAB platform, and the optimal configuration plan is obtained by iterating between the main and sub problems. The specific procedures are shown in Fig. 5.

Procedures for solving the bilevel configuration problem

1. Initialization and data input.
2. Obtain the typical scenario set S_3 in *Section 3.2.1*.
3. Set the iteration number $kk=1$, the lower bound $C_{total}^{\min(1)}=-\infty$, and give the initial decision value of main problem $x_{up}^{(1)}$;
4. **For** $\left|C_{total}^{\max(kk)}-C_{total}^{\min(kk)}\right|>\varepsilon$

    Sub problem: Seeking the optimal operation scheme.

    1. Receive x_{up} from the **main problem**.
    2. Call **Gurobi** solver to get the optimal scheduling scheme based on **SADMM** (36) ;
    3. **Return** optimal solution of sub problem $x_{low}^{(kk)}$, Benders cut constraints (31),(33) and update the upper bound $C_{total}^{\max(kk)}$;
    4. **End procedure**

5. **Optimality test of solution**
6. **If** $\left|C_{total}^{\max(kk)}\text{-}C_{total}^{\min(kk)}\right|\le\varepsilon$ **then** stop the iteration;
7. **Else** $kk=kk+1$, continue main problem solving

    Main problem: Seeking the optimal configuration plan.

    1. Receive $x_{low}^{(kk)}$ and Benders cut constraints from the **sub problem**.
    2. Call **Gurobi** solver to get the optimal configuration plan (34) ;
    3. **Return** optimal solution of main problem $x_{up}^{(kk+1)}$, and update the lower bound $C_{total}^{\min(kk+1)}$;
    4. **Continue** sub problem solving

8. **End**
9. **End**
10. **Output** the optimal configuration plan.
11. **End procedure**

Fig.5 Procedure of model solving

4. Case study

4.1 Case description

In this section, based on a practical project of "Energy Internet Town in Xiong'an New Area" in China, which is shown in Fig. 6, Area A is selected for case studies to configure a MES with three communities (I, II, III), and its structure diagram is shown in Fig. 7. Due to the differentiated resource and demand conditions, the structures of community II and III are similar to that of community I in Fig. 3, but there are no HS configuration and heating demand in II, and no HS/CS configurations and gas demand in III, and gas air conditioner (GC) is configured instead of AC in III. In this paper, only energy production equipment are chosen to be additionally configured. PV and WT are quantity configuration items, while the rated capacities of a single WT and PV are 20kW and 10kW, respectively. Other energy equipment are capacity configuration items, while the optimization step for capacity configuration is set to be 10 kW/kWh. Moreover, this work only considers the communities have interaction pipelines or not, which are set as 0-1 variables. The total number of days in a year is taken as 365, including 183 days in transitional season, 92 days in summer and 90 days in winter. Load power, light intensity and wind speed curves on typical days are shown in Fig. A1. The equipment parameters and DR parameters are listed in Table A1-A4, collected from [21], [28] and [33], and energy prices are given in Table A5.

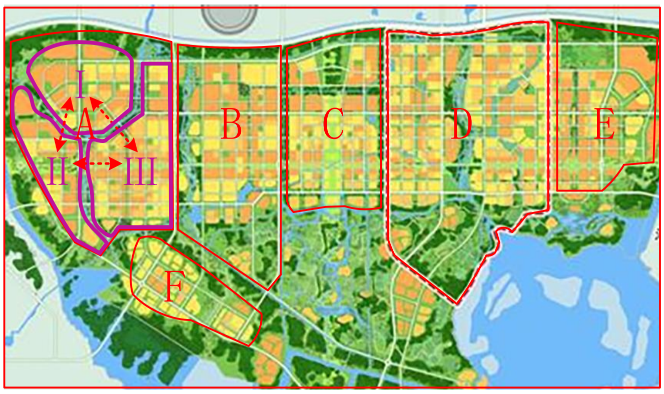

Fig.6 Practical MES planning case of Xiong'an New Area

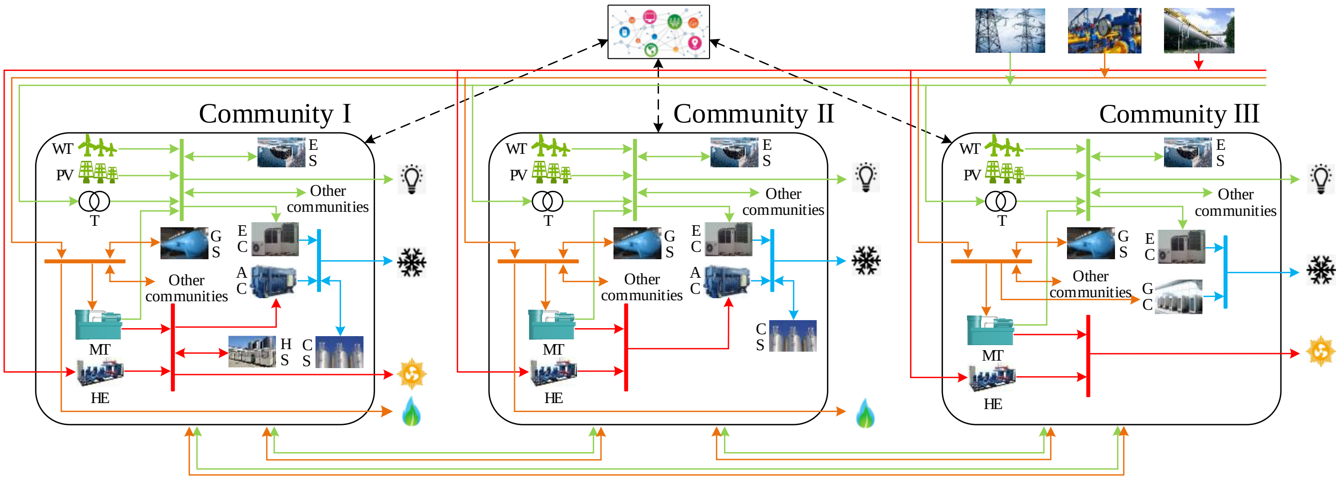

Fig.7 Structure diagram of multi-community MES

4.2 Simulation results and discussion

4.2.1 Configuration results analysis

Based on the proposed model, the quantity and capacity configuration results of the MES with multi communities are listed in Table 1, and Fig. 8 shows the comparison of investment cost items. It is noted that the basic configuration quantity and total basic capacity correspond to the numbers on the left of "+", and the shared configuration quantity and total shared capacity correspond to the number on the right of "+".

Combined with the upper configuration limits of energy production equipment in Table A3, it can be seen that the configuration quantity of PV and WT in communities I-III have all reached the maximum basic quantity limits, which are 15/10/6 and 5/3/2, and the maximum additional quantity limits, which are 4/2/0 and 1/0/0, respectively. It is because PV and WT can effectively relieve the pressure of energy consumption to a certain extent and further reduce the operation cost, therefore, communities prefer to configure more energy production equipment for reasons of planning economy. Moreover, from the view of different energy equipment types, Fig. 8 shows that energy production part accounts for the largest proportion of investment cost, followed by energy conversion, sharing and storage parts. In addition, there are interaction pipeline configurations among the three communities, and additional capacity sharing equipment (refer to PV and WT) are configured in both community I and II, reflecting that the communities prefer to adopt the sharing measures for better configuration scheme. The results show that the proposed strategy can reasonably achieve multi-community planning in consideration of capacity and energy sharing, and further improving the economics and flexibility of MES planning.

Table.1 Quantity/Capacity configuration results of MESs

Community	Energy production		Energy conversion				Energy storage				Energy sharing
	PV (Number/kW)	WT (Number/kW)	MT (kW)	EC (kW)	AC (kW)	GC (kW)	ES (kWh)	GS (kWh)	HS (kWh)	CS (kWh)	Interaction pipelines
I	(15+4)/ (150+40)	(5+1)/ (100+20)	80	180	250	--	50	100	50	200	√
II	10+2/ (100+20)	(3+0)/ (60+0)	100	250	250	--	50	100	--	100	√
III	6+0/ (60+0)	(2+0)/ (40+0)	110	140	--	260	90	140	--	--	√

Table.2 Detailed composition of MES planning costs (Million ¥)

	Investment cost	Fixed maintenance cost	Residual value	Purchase cost	Operational maintenance cost	Environmental cost	Demand response cost	Transmission loss cost	Total annual cost
MES	0.7605	0.1787	-0.0296	8.2990	0.2342	0.3260	0.9949	0.0142	10.7779

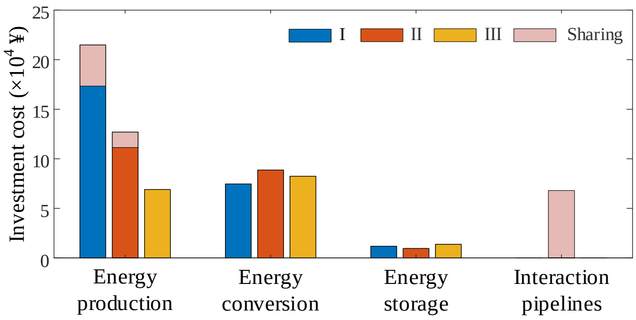

Fig. 8. Comparison chart of investment cost items

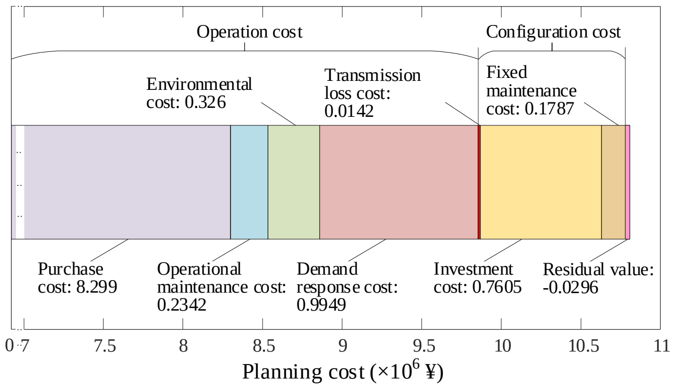

Fig. 9. Detailed composition of MES planning costs (Million ¥).

Table 2 and Fig. 9 give the detailed composition of MES planning cost. It is noted that the planning cost consists of configuration and operation costs, while the former includes investment cost, fixed maintenance cost and equipment residual value, the latter consists of purchase cost, operational maintenance cost, environmental cost, demand response cost and transmission loss cost. It is shown that the total annual cost of MES planning is optimized to be ¥10.7779 million, of which the standard deviation (STD) is calculated to be ¥0.0327 million. The purchase cost accounts for the largest proportion, which is about 77%, mainly followed by demand response and investment costs, which are 9.23% and 7.06% respectively. Combined with the above analysis, it can be seen that the configuration results are derived from multi factors, reflected in following aspects.

1) The proposed strategy aims at the best economy to obtain the optimal MES configuration scheme, including considerations over multi configuration and operation cost items. The CO2 emissions and demand response compensations are treated as economic costs and added to the MES planning cost, which reflects that the economy, carbon emission and user benefit items have been taken into account in the proposed strategy.
2) The configuration results are developed on the basis of hierarchical planning framework, which jointly considers the multi-dimension sharing, uncertainty addressing and demand response, and obtains the best configuration scheme through the collaborative optimization of both planning and operation stages.

4.2.2 Operation results analysis

Based on the configuration scheme given in Table 1, the operation strategy of MES is optimized. Take the community I for example, the energy supply and demand scheduling results on a typical day of transitional season are shown in Fig. 10, while the energy supply and demand are described above and below the horizontal axis, respectively. In combination with the energy prices and prediction curves, Fig. 10 is further analysed as follows. Regarding the electric power scheduling results shown in Fig. 10(a), the community prefers to perform electricity purchases to meet the power demand in periods of low prices (23:00-07:00), while the shortage is alleviated by MT and WT; in periods of high prices (08:00-22:00), MT output increases as the share of electricity purchase decreases, and the shortage is satisfied by PV, WT, ES and other communities. For the gas scheduling results in Fig. 10(b), the gas demand, including load and MT, is mainly satisfied by purchases, while the shortage is supplied by GS and other communities. Regarding the heat and cooling power scheduling results in Figs. 10(c) and (d), the heating demand of load and AC is supplied by heat purchases, MT and HS, and the cooling demand is satisfied by EC, AC, and CS. Moreover, the proportion of AC output goes up with the increase of electricity prices in periods of 8:00-22:00, while the thermal output of MT also increases accordingly to cover the heating demand of AC.

As discussed above, it is seen that community I can achieve the multi energy supply and demand balance, which is based on the improved energy hub model established in Section 2.2, and the operation results stem from the combined effects of following factors: 1) The configuration scheme is obtained in consideration of capacity sharing among communities, which effectively provides supports for the optimal operation and energy balance of MES; 2) Taking the economy, carbon emissions and user benefits into account, various energy equipment are fully coordinated to meet the diversified energy demands of users; 3) The adopted stochastic-robust-based scenarios are obtained to address the source-load uncertainties to improve the accuracy of scheduling plan, and the shifted, replaced and interrupted DR measures are jointly considered to promote the energy balance from the perspectives of time and energy vectors; 4) Given the multi-dimension sharing measures, electricity and gas interactions are introduced into MES operation to further promote the energy balance of multi communities.

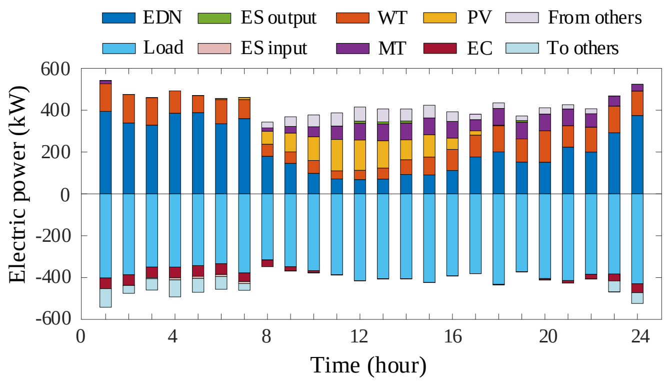

(a) Electric power.

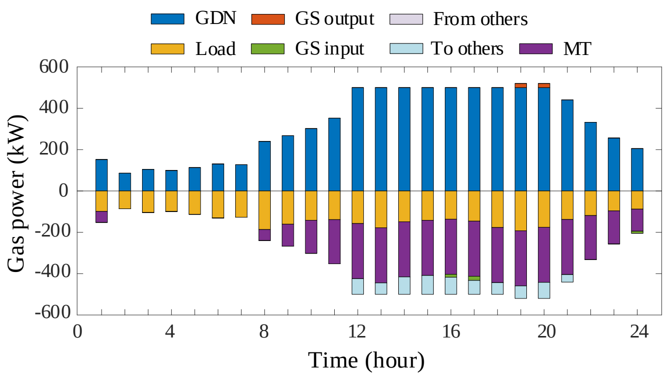

(b) Gas power.

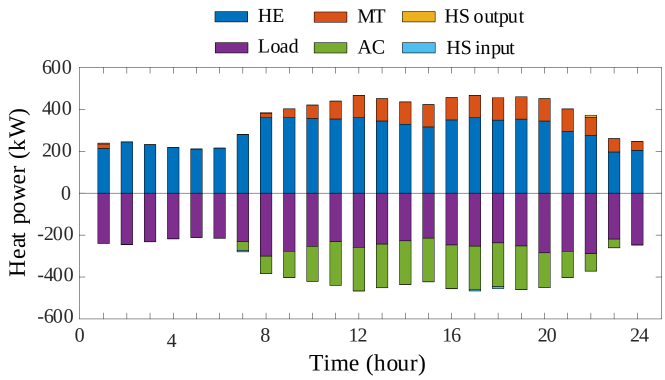

(c) Heat power.

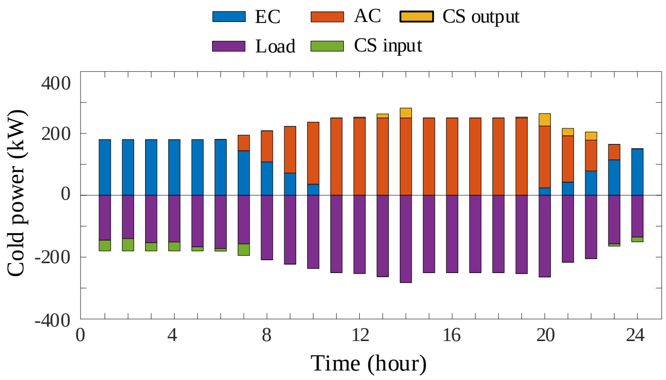

(d) Cold power.

Fig.10 Energy supply and demand scheduling results of residential community in day-ahead stage

Fig. 11 gives the energy interaction results among communities, and the interactions comprise two parts: traded power interactions related to basic equipment configuration capacity, and shared power interactions related to additional equipment configuration capacity from capacity sharing. The energy outputs and inputs of community are shown above and below the horizontal axis, respectively. One can observe that electricity interactions are mainly divided into two periods: from community I to II during 23:00-7:00 (traded + shared power), and from community II to I during 8:00-22:00 (shared power). Similarly, the gas interactions mainly occur during 12:00-21:00, which are from community I to II and III. This is due to the different source-load characteristics and curve trends of the three communities. First, the shared capacity is reasonably allocated to multi communities according to their energy supply and demand conditions, and then the energy interactive scheduling among communities is further performed. Moreover, one can choose to sell energy to others to gain more benefits when it is in low load periods, while others are also willing to perform an energy purchase to meet user demands and reduce operation costs. Therefore, the adoption of energy sharing measures is conductive to improving the operation economy and flexibility, further promoting the energy supply and demand balance.

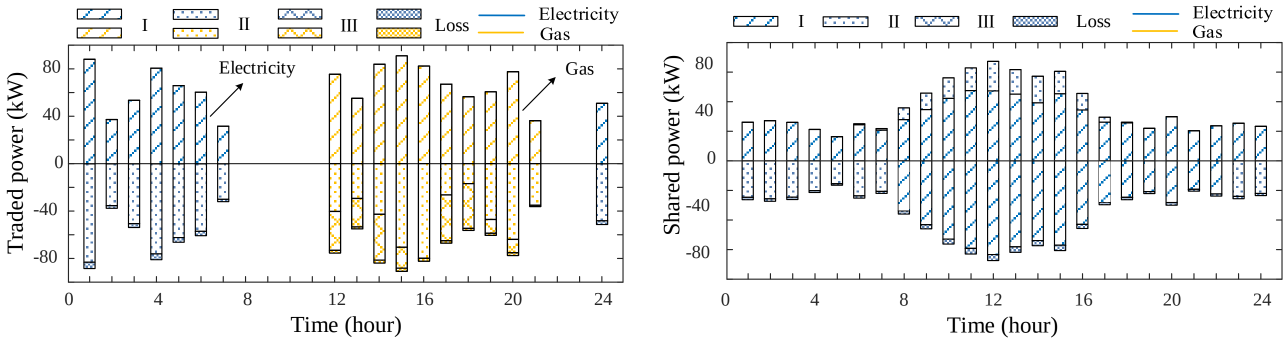

(a) Traded power (b) Shared power

Fig.11 Energy interaction results among communities

4.2.3 Comparative analysis

To further verify the effectiveness and advantages of the bilevel coordinated configuration strategy developed in this paper, four cases are simulated based on the MES project. The detailed case descriptions are given below, and the simulation results for MES planning costs are summarized in Table 3.

Case 1: Traditional bilevel planning framework [12];

Case 2: Union configuration with electricity sharing [26];

Case 3: Bilevel coordinated planning in the paper but with no sharing considered;

Case 4: Bilevel coordinated planning with multi-dimension sharing considered, proposed in this paper.

Table.3 Composition of MES planning costs in different cases (Million ¥)

Case	Investment cost	Fixed maintenance cost	Residual value	Operation cost	Total annual cost
Case 1	0.6516	0.1515	-0.0257	10.6247	11.4021
Case 2	0.6838	0.1606	-0.0266	10.5548	11.3726
Case 3	0.6253	0.1463	-0.0245	10.1885	10.9356
Case 4	0.7605	0.1787	-0.0296	9.8683	10.7779

It can be seen from Table 3 that compared with case 1, which offers a general bilevel planning framework, case 2, which proposes a union optimal configuration strategy with electricity sharing, and case 3, which adopts the bilevel coordinated planning strategy with no sharing considered, the total annual cost of case 4 with the proposed strategy is the lowest, which is ¥10.7779 million and decreases by ¥0.6242 million, ¥0.5947 million and ¥0.1577 million. Specifically, the proposed strategy possesses a higher configuration cost and lower operation cost compared with compared ones, which also indicates in a way that, a higher capacity configuration of renewable energy sources is adopted and operation economy is also improved owing to the MES sharing measures. Therefore, the proposed strategy could also contribute to better RES utilizations and consumptions. Moreover, the reference cases do not consider the sharing methods on the planning, operation and information levels, and cases 1 and 2 lack the consideration of equipment residual values, demand response and more effective source-load scenarios in the modeling, as shown in Table 4. In summary, the proposed strategy is based on the hierarchical planning framework, which coordinately introduces multi-dimension sharing, multi uncertainties addressing and multi demand response measures into the bilevel configuration of MESs. It exhibits better performances in terms of reducing MES planning costs and reasonably taking into account the planning economy, robustness, carbon emissions and user benefits.

Table.4 Qualitative comparison results of some considered factors

Case	Community sharing	Demand response	Uncertainty addressing	Environment protection	Residual values
Case 1	—	—	—	√	—
Case 2	Only electricity sharing	—	Stochastic optimization	√	—
Case 3	—	√	Stochastic-robust combined optimization	√	√
Case 4	Multi-dimension sharing	√	Stochastic-robust combined optimization	√	√

5. Conclusion

A coordinated configuration strategy is proposed for a multi-community MES based on multi-dimension sharing. Configuration and operation results analysis, as well as comparative analysis are carried out in case studies to demonstrate the effectiveness and advantages of the proposed strategy. Based on the simulation results, the conclusions can be summarized as follows:

1) The improved energy hub model coordinates multi energy carriers, uncertainties, demand response and sharing measures, which is generic and applicable for the community-level MES, and can provide guidance for the configuration and operation of MES.
2) The proposed strategy jointly considers capacity, energy and information sharing measures in both the planning and operation stages,which can improve system flexibility and further promote the energy supply and demand balance by multi-community interactions, thus effectively reducing MES configuration redundancy and planning costs.
3) The bilevel configuration model is solved by a decomposition method combined with SADMM and validated by a typical town case in China. The effectiveness and advantages of the proposed strategy are verified after configuration and operation results analysis, as well as comparative analysis with related studies.
4) The simulation results show that the proposed model (case 4) possesses better economic performance than a traditional bilevel planning model (case 1), a union configuration model with electricity sharing (case 2) and a bilevel coordinated planning model without sharing methods (case 3). Compared with the reference cases, the proposed model contributes to a decrease in the total planning cost, by ¥0.6242 million, ¥0.5947 million and ¥0.1577 million, which are approximately 5.47%, 5.23% and 1.44%, respectively. In addition, the proposed strategy achieves a better consideration of planning economy, robustness, carbon emissions and user benefits.
5) In our current study, we mainly focus on the quantity and capacity configuration for MESs planning, however, the specifications and types of equipment and pipelines have not been taken into account, and only energy production equipment are considered for capacity sharing, while the above may have an impact on the application of the planning scheme. In future work, it would be more interesting and useful to extend the capacity sharing to equipment of other energy parts, and further incorporate the equipment type and specification configuration into the MESs planning.

Appendix

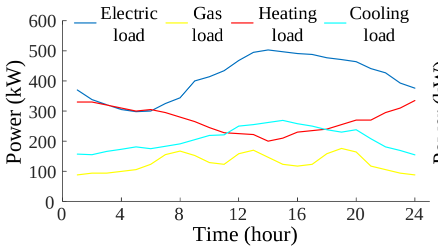

(a) Typical day of transitional season (I)

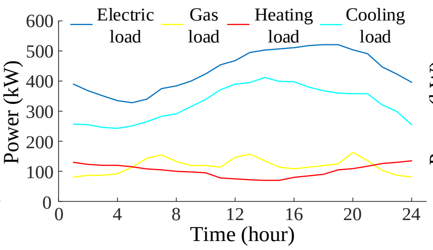

(b) Typical day of summer (I)

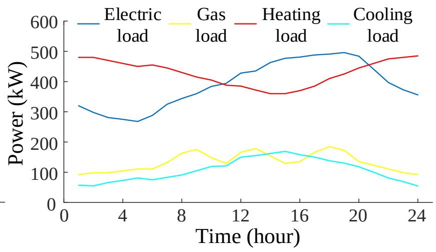

(c) Typical day of winter (I)

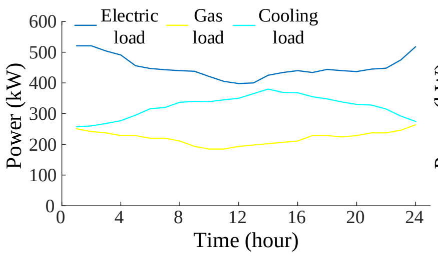

(d) Typical day of transitional season (II)

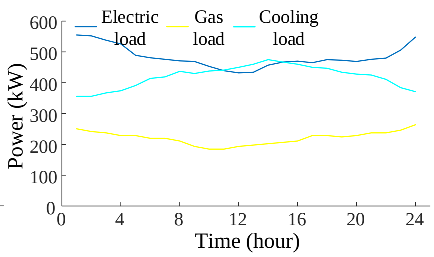

(e) Typical day of summer (II)

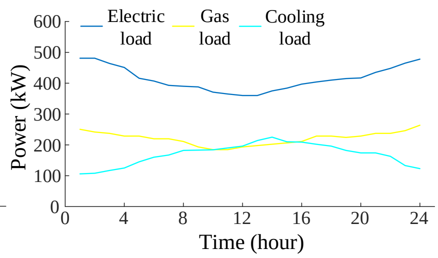

(f) Typical day of winter (II)

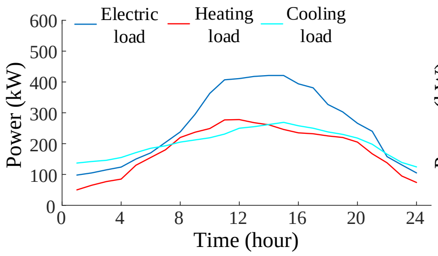

(g) Typical day of transitional season (III)

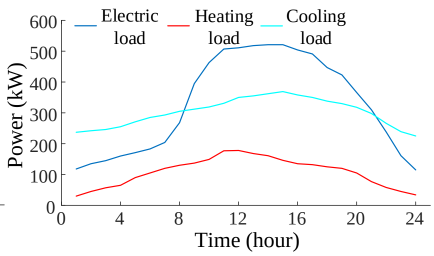

(h) Typical day of summer (III)

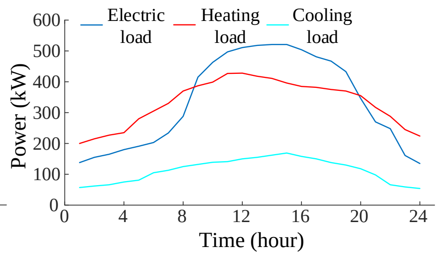

(i) Typical day of winter (III)

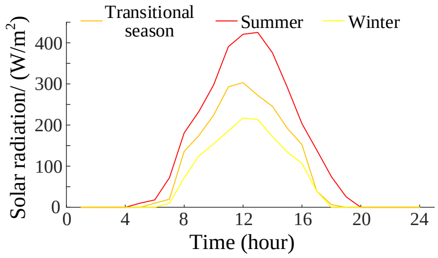

(j) Solar radiation on typical days

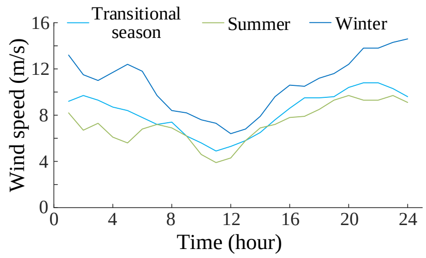

(k) Wind speed on typical days

Fig.A1 Load power, solar radiation and wind speed curves on typical days.

The detailed EH model is expressed as below:

$$L = \begin{bmatrix} \eta_t & 0 & 0 \\ 0 & 1 & 0 \\ 0 & 0 & \eta_{he} \\ 0 & 0 & 0 \end{bmatrix} \cdot \begin{bmatrix} P_b \\ G_b \\ H_b \end{bmatrix} + \begin{bmatrix} P_{pv} + P_{wt} \\ 0 \\ 0 \\ 0 \end{bmatrix} + \begin{bmatrix} \eta_{mt}^{ge} H_{ng} & -1 & 0 \\ -1 & 0 & 0 \\ \eta_{mt}^{gh} H_{ng} & 0 & -1 \\ 0 & \eta_{ec} & \eta_{ac} \end{bmatrix} \cdot \begin{bmatrix} G_{mt} \\ P_{ec} \\ H_{ac} \end{bmatrix}$$
$$+ \begin{bmatrix} 1 & -1 & 0 & 0 & 0 & 0 & 0 & 0 \\ 0 & 0 & 1 & -1 & 0 & 0 & 0 & 0 \\ 0 & 0 & 0 & 0 & 1 & -1 & 0 & 0 \\ 0 & 0 & 0 & 0 & 0 & 0 & 1 & -1 \end{bmatrix} \cdot \begin{bmatrix} P_{es,d} \\ P_{es,c} \\ P_{gs,d} \\ P_{gs,c} \\ P_{hs,d} \\ P_{hs,c} \\ P_{cs,d} \\ P_{cs,c} \end{bmatrix} \tag{A1}$$

where P_b, G_b and H_b are the and are the electric, gas and heating power purchases, respectively; P_{pv} and P_{wt} are the output power of PV and WT; P_{ec}, G_{mt} and H_{ac} are the corresponding power consumptions of MT, EC and AC; $P_{es/gs/hs/cs,c}$ and $P_{es/gs/hs/cs,d}$ are the charging and discharging power of multi energy storage equipment; H_{ng} is the low heating value of gas, set as 9.7 kWh/m^3 in this paper; η_t and η_{he} denote the conversion efficiencies of T and HE; η_{mt}^{ge} and η_{mt}^{gh} denote the gas-electric and gas-heat efficiencies of MT; η_{ec} and η_{ac} denote the cooling efficiencies of EC and AC, respectively.

Tab.A1 Parameters of energy storage

Type	Upper charging limit	Upper discharging limit	Upper storage state	Lower storage state	Charging efficiency	Discharging efficiency	Loss efficiency
ES	0.2	0.2	0.9	0.1	0.9	0.9	0.001
GS	0.2	0.2	0.9	0	0.95	0.95	0.001
HS	0.2	0.2	0.9	0	0.88	0.88	0.01
CS	0.2	0.2	0.9	0	0.88	0.88	0.01

Tab.A2 Parameters of other energy equipment

Energy equipment	Unit investment cost (¥/(kW/kW h))	Operational maintenance coefficient (¥/kWh)	Capacity limits (kW/kWh)	Rated capacity (kW/kWh)	Efficiency	Life cycle (year)
T	—	—	—	—	1	—
HE	—	—	—	—	0.9	—
PV	10000	0.025	—	10	—	30
WT	4000	0.0296	—	20	—	20
EC	828	0.02	0~250	—	3.5	20

AC	1127	0.01	0~250	—	1.2	20
GC	989	0.025	0~300	—	1.5	20
MT	5230	0.0352	0~200	—	Electric: 0.3 Heat: 0.4	25
ES	1000	0.0018	50~200	—	—	10
GS	90	0.001	50~200	—	—	20
HS	102	0.0016	50~200	—	—	20
CS	190	0.0014	50~200	—	—	20

Tab.A3 Other parameters of MESs planning

Parameter	Value	Parameter	Value	Parameter	Value	Parameter	Value
α	0.031 ¥/kg	γ_e / γ_g	0.06/0.03	δ_{re}^{obj}	8%	ε_f^{obj}	2%
β_{mt}	0.724 kg/kWh	β_p	0.972 kg/kWh	β_g	0.23 kg/kWh	β_h	0.845 kg/kWh
r	6.7%	λ^e / λ^g	1800/950 ¥/m	z^e / z^g	30/20 years	l_{ij}^e / l_{ij}^g	100 m
$K_{1,b,\max}^{PV}$	15	$K_{1,b,\max}^{WT}$	5	$K_{1,a,\max}^{PV}$	4	$K_{1,a,\max}^{WT}$	1
$K_{2,b,\max}^{PV}$	10	$K_{2,b,\max}^{WT}$	3	$K_{2,a,\max}^{PV}$	2	$K_{2,a,\max}^{WT}$	0
$K_{3,b,\max}^{PV}$	6	$K_{3,b,\max}^{WT}$	2	$K_{3,a,\max}^{PV}$	0	$K_{3,a,\max}^{WT}$	0
$P_{i,buy,\max}$	400 kW	$G_{i,buy,\max}$	500 kW	$H_{i,buy,\max}$	400 kW	$P_{e,ij,\max} / P_{g,ij,\max}$	100 kW

Tab.A4 DR parameters

Parameter	Value	Parameter	Value	Parameter	Value	Parameter	Value
$k_{e,in}$	0.1	$k_{g,in}$	0.1	$k_{h,in}$	0.1	$k_{c,in}$	0.1
$k_{e,sft}$	0.3	$k_{g,sft}$	0.4	$k_{h,sft}$	0	$k_{c,sft}$	0
$k_{e,rpl}$	0.2	$k_{g,rpl}$	0.2	$k_{h,rpl}$	0.3	$k_{c,rpl}$	0.3
Proportion of fixed electric load	0.4	Proportion of fixed gas load	0.3	Proportion of fixed heating load	0.6	Proportion of fixed cooling load	0.6
k_{eg}	1.5	k_{ec}	3.2	k_{eh}	2.8	k_{gc}	1.4
k_{gh}	1.6	k_{hc}	0	$p_{e,sft}$	0.8 ¥/kWh	$p_{g,sft}$	0.35 ¥/kWh
$p_{e,cap}$	0.008 ¥/kWh	$p_{g,cap}$	0.0035 ¥/kWh	$p_{h,cap}$	0.0025 ¥/kWh	$p_{c,cap}$	0.0025 ¥/kWh
$p_{u,in}$	Real-time energy price	$L_{e,sft,\max}^t$	$0.3\,\overline{L}_e^t$	$L_{g,sft,\max}^t$	$0.4\,\overline{L}_g^t$	$L_{u,in,\max}^t$	$0.1\,\overline{L}_u^t$
$L_{e,rpl,\max}^t$	$0.2\,\overline{L}_e^t$	$L_{g,rpl,\max}^t$	$0.2\,\overline{L}_g^t$	$L_{h,rpl,\max}^t$	$0.3\,\overline{L}_h^t$	$L_{c,rpl,\max}^t$	$0.3\,\overline{L}_c^t$

Tab.A5 Energy prices

Time (h)	Electric power (¥/kWh)		Gas power (¥/kWh)		Heating power (¥/kWh)
	$\overline{p}_e^t$	p_e^t	$\overline{p}_g^t$	p_g^t	p_h^t
1	0.48	0.32	0.35	0.29	0.28
2	0.48	0.28	0.35	0.31	0.28
3	0.48	0.26	0.35	0.31	0.28
4	0.48	0.25	0.35	0.32	0.28
5	0.48	0.25	0.35	0.34	0.28
6	0.48	0.25	0.35	0.29	0.28
7	0.48	0.27	0.35	0.37	0.20
8	0.88	0.82	0.35	0.41	0.20
9	0.88	0.93	0.35	0.37	0.20
10	0.88	0.96	0.35	0.30	0.20
11	0.88	1.00	0.35	0.29	0.20
12	1.10	1.32	0.35	0.48	0.20
13	1.10	1.39	0.35	0.50	0.20
14	1.10	1.40	0.35	0.45	0.20
15	0.88	1.15	0.35	0.29	0.20
16	0.88	1.16	0.35	0.27	0.20
17	0.88	1.18	0.35	0.29	0.20
18	0.88	1.18	0.35	0.38	0.20
19	1.10	1.40	0.35	0.50	0.28
20	1.10	1.40	0.35	0.50	0.28

21	1.10	1.38	0.35	0.37	0.28
22	1.10	1.26	0.35	0.32	0.28
23	0.48	0.38	0.35	0.31	0.28
24	0.48	0.35	0.35	0.29	0.28

Acknowledgements

This work was supported by the National Natural Science Foundation of China under Grant 52177084 and the North China Electric Power University Scholarship Fund.

References

[1] Rifkin J. The third industrial revolution: how lateral power is transforming energy, the economy, and the world [M]. New York: Palgrave MacMillan, 2011: 24-71.

[2] Erixno O, Rahim N A, Ramadhani F, Adzman N N. Energy management of renewable energy-based combined heat and power systems: A review [J]. Sustainable Energy Technologies and Assessments, 2022, 51: 101944.

[3] National Development and Reform Commission, National Energy Administration. Energy technology revolution innovation action plan (2016-2030) [OL]. 2016. Available: http://zfxxgk.ndrc.gov.cn/web/iteminfo.jsp?id=2491.

[4] Greisen Christoffer. EnergyLab Nordhavn, integrated energy infrastructures and smart components [C] // DTU Sustain Conference 2015, 2015, Copenhagen, Denmark.

[5] Congress of United States. Energy independence and security ACT of 2007 [OL]. 2007, Available: https://www.congress.gov/110 /plaws/publ140/PLAW-110publ140.pdf.

[6] Wu J, Yan J, Jia H, Hatziargyriou N, Sun H. Integrated energy systems[J]. Applied Energy, 2016, 167: 155-157.

[7] Geidl M, Koeppel G, Favreperrod P, Klockl B, Andersson G, Frohlich K. Energy hubs for the future[J]. IEEE Power and Energy Magazine, 2007, 5(1): 24-30.

[8] Wang Y, Zhang N, Kang C, Daniel S K, Yang J, Xia Q. Standardized matrix modeling of multiple energy systems[J]. IEEE Transactions on Smart Grid, 2019, 10(1): 257-270.

[9] Chen B, Sun H, Wu W, Guo Q, Qiao Z. Energy circuit theory of integrated energy system analysis (III): steady and dynamic energy flow calculation [J]. Proceedings of CSEE, 2020, 40(15): 4820-4830.

[10] Li C, Yang H, Shahidehpour M, Xu Z, Zhou B, Cao Y, et al. Optimal planning of islanded integrated energy system with solar-biogas energy supply[J]. IEEE Transactions on Sustainable Energy, 2020, 11(4): 2437-2448.

[11] Petkov I, Mavromatidis G, Knoeri C, Allan J, Hoffmann V H. MANGOret: An optimization framework for the long-term investment planning of building multi-energy system and envelope retrofits [J]. Applied Energy, 2022, 314: 118901.

[12] Ma T, Wu J, Hao L, Lee W J, Yan H, Li D. The optimal structure planning and energy management strategies of smart multi energy systems [J]. Energy, 2018, 160: 122-141.

[13] Barros E G D, Aken B B V, Burgers A R, Slooff-Hoek L H, Fonseca R M. Multi-Objective optimization of solar park design under climatic uncertainty [J]. Solar Energy, 2022, 231: 958-969.

[14] Ho C O, Nie T, Su L, Yang Z, Schwegler B, Calvez P. Graph-based algorithmic design and decision-making framework for district heating and cooling plant positioning and network planning [J]. Advanced Engineering Informatics, 2021, 50: 101420.

[15] O'Malley M J, Anwar M B, Heinen S, Kober T, McCalley J, McPherson M, et al. Multicarrier energy systems: shaping our energy future[J]. Proceedings of the IEEE, 2020, 108(9): 1437-1456.

[16] Cao Y, Wei W, Wang J, Mei S, Shafie-Khah M, Catalao J. Capacity planning of energy hub in multi-carrier energy networks: a data-driven robust stochastic programming approach[J]. IEEE Transactions on Sustainable Energy, 2020, 11(1): 3-14.

[17] Gong J, Li Y, Lv J, Huang G, Suo C, Gao P. Development of an integrated bi-level model for China's multi-regional energy system planning under uncertainty [J]. Applied Energy, 2022, 308: 118299.

[18] Bahrami S, Sheikhi A. From demand response in smart grid toward integrated demand response in smart energy hub[J]. IEEE Transactions on Smart Grid, 2016, 7(2): 650-658.

[19] Mansouri S A, Ahmarinejad A, Sheidaei F, Javadi M S, Jordehi A R, Nezhad A E, et al. A multi-stage joint planning and operation model for energy hubs considering integrated demand response programs [J]. International Journal of Electrical Power & Energy Systems, 2022, 140:108103.

[20] Xiang Y, Cai H, Gu C, Shen X. Cost-benefit analysis of integrated energy system planning considering demand response[J]. Energy, 2020, 192: 116632.

[21] Li P, Wang Z, Wang N, Yang W, Li M, Zhou X, et al. Stochastic robust optimal operation of community integrated energy system based on integrated demand response[J]. International Journal of Electrical Power & Energy Systems, 2021, 128:106735.

[22] Wang N, Heijnen P W, Imhof P J. A multi-actor perspective on multi-objective regional energy system planning [J]. Energy policy, 2020, 143: 111578.

[23] Horasan M B, Kilic H S. A multi-objective decision-making model for renewable energy planning: The case of Turkey [J]. Renewable Energy, 2022, 193: 484-504.

[24] Li Y, Gao B, Qin Y, Chen N. A hierarchical multi-objective capacity planning method for distributed energy system considering complementary characteristic of solar and wind [J]. Applied Energy, 2022, 141:108200.

[25] Gan W, Yan M, Wen J, Yao W, Zhang J. A low-carbon planning method for joint regional-district multi-energy systems: From the perspective of privacy protection [J]. Applied Energy, 2022, 311: 118595.

[26] Li P, Wu D, Li Y, Yin Y, Fang Q, Chen B. A multi-objective union optimal configuration strategy for multi-microgrid integrated energy system considering bargaining game [J]. Power System Technology, 2020, 44(10): 3680-3690.

[27] Pan G, Gu W, Zhou S, Wu Z, Lu Y. Synchronously decentralized adaptive robust planning method for multi-stakeholder integrated energy systems[J]. IEEE Transactions on Sustainable Energy, 2020, 11(3): 1128-1139.

[28] Li P, Wang Z, Wang J, Guo T, Yin Y. A multi-time-space scale optimal operation strategy for a distributed integrated energy system [J]. Applied Energy, 2021, 289: 116698.

[29] Cui S, Wang Y W, Xiao J W. Peer-to-peer energy sharing among smart energy buildings by distributed transaction[J]. IEEE Transactions on Smart Grid, 2019, 10(6): 6491-6501.

[30] Xu X, Li J, Xu Y, Lai C. A two-stage game-theoretic method for residential PV panels planning considering energy sharing mechanism[J]. IEEE Transactions on Power Systems, 2020, 35(5): 3562-3573.

[31] Zhang Y, He Y, Yan M, Guo C, Ding Y. Linearized stochastic scheduling of interconnected energy hubs considering integrated demand response and wind uncertainty[J]. Energies, 2018, 11(9): 2448.

[32] Zhao J, Zhang Y, Liu Z, Hu W, Su D. Distributed multi-objective day-ahead generation and HVDC transmission joint scheduling for two-area HVDC-linked power grids[J]. International Journal of Electrical Power & Energy Systems, 2022, 134: 107445.

[33] Li P, Wang Z, Liu H, Wang J, Guo T, Yin Y. Bi-level optimal configuration strategy of community integrated energy system with coordinated planning and operation [J]. Energy, 2021, 236: 121539.